Briefs

Channel Noise Modeling of Deep Submicron MOSFETs

Chih-Hung Chen and M. Jamal Deen

***Abstract*—This brief presents a new channel noise model using the channel length modulation (CLM) effect to calculate the channel noise of deep submicron MOSFETs. Based on the new channel noise model, the simulated noise spectral densities of the devices fabricated in a 0.18 μm CMOS process as a function of channel length and bias condition are compared to the channel noise directly extracted from RF noise measurements. In addition, the hot electron effect and the noise contributed from the velocity saturation region are discussed.**

***Index Terms*—Channel length modulation, channel noise of deep submicron MOSFETs, diffusion noise, high-frequency noise modeling, thermal noise.**

I. Introduction

In addition to the high levels of integration for digital circuit design offered by advanced CMOS processes, these MOSFETs are also capable of operating in the GHz regime because of their very high unity-gain frequencies of tens of GHz. Because of this, MOSFETs have become very attractive for RF IC applications [1]. However, when working at high frequencies, the noise generated within the device itself will play an increasingly important role in the overall RF IC performance, for example in the noise performance of a front-end receiver in an RFIC. Therefore, a physics-based noise model which can accurately predict the noise characteristics of deep-submicron MOSFETs is crucial for the low noise, RF IC design.

To date, there are many publications on the noise modeling of the channel noise which is the most dominant noise source in short-channel MOSFETs [2]–[11]. The noise model based on the Nyquist theory and the dc model of MOSFETs successfully predicted the channel noise devices working the linear region. However, for RFICs, the short-channel MOSFETs usually operate in the saturation region for most applications, and it is often observed that the channel noise generated from the short-channel devices is higher than expected from the conventional channel noise theory for long-channel MOSFETs [7], [10]. Some approaches have been presented to explain the discrepancy by introducing the extra channel noise from the velocity saturation through either the hot-electron effect [10] or the diffusion noise [9], [12]. The noise from the saturation region proposed in these models is neither physical nor proven by the measured noise data of deep-submicron MOSFETs. In this brief, a new analytical noise model using the channel length modulation (CLM) effect to calculate the channel noise of deep submicron MOSFETs is presented and verified with the measured data obtained using the direct extraction method [13], [14]. In addition, the hot electron effect and the noise from the velocity saturation region are discussed.

Manuscript received February 12, 2002; revised April 9, 2002. This work was supported in part by grants from Conexant Systems, Inc., Newport Beach, CA, Micronet, and the Natural Sciences and Engineering Research Council (NSERC) of Canada. The review of this brief was arranged by Editor C.-Y. Liu.

The authors are with the Electrical and Computer Engineering, McMaster University, Hamilton, ON L8S 4K1 Canada (e-mail: chench@mcmaster.ca; jamal@mcmaster.ca).

Publisher Item Identifier 10.1109/TED.2002.801229.

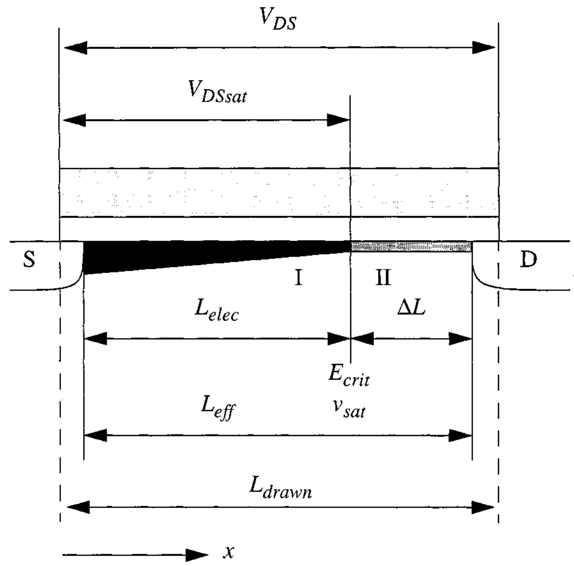

Fig. 1. Cross section of a MOSFET channel divided into a gradual channel region (I) and a velocity saturation region (II).

II. Calculation of Channel Noise in MOSFETs

The approach used in this paper to calculate the channel noise is based on a two–section channel model in which the channel of a MOSFET is divided into two regions: a gradual channel region of length $L_{elec} = L_{eff} - \Delta L$ (region I in Fig. 1) and a velocity saturation region of length ΔL (region II in Fig. 1) [4], [10], [15]. In this brief, ΔL is given by [16]

$$\Delta L = \frac{1}{\alpha} \ln \left(\frac{\alpha (V_{DS} - V_{DSsat}) + E_D}{E_{crit}} \right) \tag{1}$$

where

$$E_D = E_{crit} \sqrt{1 + \left(\frac{\alpha (V_{DS} - V_{DSsat})}{E_{crit}} \right)^2} \tag{2}$$

and

$$\alpha = \lambda \sqrt{\frac{3}{2} \frac{C_{ox}}{x_j \varepsilon_{si} \varepsilon_o}}. \tag{3}$$

Here, E_{crit} is the critical lateral electric field at which carriers travel at their saturation velocity, x_j is the junction depth of the source and drain regions, C_{ox} is the gate-oxide capacitance per unit area, and λ is a fitting parameter to adjust the channel length modulation and it is unity in this work. Based on this channel model, the total noise current shown at the drain terminal will be the sum of the noise current contributed from both regions.

A. Channel Noise From the Gradual Channel Region (Region I)

In the derivation of the channel noise in the gradual channel region, we assume that the electric field in the x direction for most of the sections in the gradual channel region is much less than the critical field E_{crit} (for example, see [17, Fig. 6(b)]). We will verify and discuss this assumption for the modeling of channel noise with the measured noise data in the next section. Using this assumption and the dc model of

MOSFETs, then the channel resistance ΔR of a section Δx at the position x_o in the gradual channel region is given by [6]

$$\Delta R(x_o) = \frac{\Delta x}{W\mu(x_o)(-Q(x_o))} \tag{4}$$

where $\mu(x_o)$ and $Q(x_o)$ are the mobility ($\mathrm{cm}^2/\mathrm{V}\cdot\mathrm{sec}$) and the electron concentration ($\mathrm{C/cm}^2$), respectively, at the position x_o. The term $-Q(x_o)$ is positive because of the negative charge $Q(x_o)$ for electrons. From the thermal noise theory (or Nyquist theory), the mean square value of the noise voltage generated from $\Delta R(x_o)$ is given by

$$\overline{\Delta v(x_o)^2} = 4kT(x_o)\Delta R(x_o)\Delta f = \frac{4kT(x_o)\Delta x \Delta f}{W\mu(x_o)(-Q(x_o))} \tag{5}$$

where k is Boltzmann's constant, $T(x_o)$ is the absolute temperature of the lattice at the position x_o, and Δf is the bandwidth. If we treat the part of the channel in the gradual channel region as a single transistor with the channel length L_{elec}, then according to the channel noise derivation presented in [6], the mean square value of the noise current $\overline{\Delta i(x_o)^2}$ delivered to the drain terminal from $\Delta R(x_o)$ is given by $\overline{\Delta v(x_o)^2}$ multiplied by the square of its local output conductance $g_{DS}(x_o)$, and $g_{DS}(x_o)$ is

$$g_{DS}(x_o) = \frac{W\mu(x_o)(-Q(x_o))}{L_{elec}}. \tag{6}$$

Assuming that the electric field in the x direction for most of the sections in the gradual channel region is much less than the critical field E_{crit}, then the local mobility $\mu(x_o)$ is about the same as the effective mobility μ_{eff} which is given by [18]

$$\mu_{eff} = \frac{\mu_o}{1 + (U_a + U_c V_{bs})\left(\frac{V_{gs}+2V_{th}}{T_{ox}}\right) + U_b\left(\frac{V_{gs}+2V_{th}}{T_{ox}}\right)^2} \tag{7}$$

where T_{ox} is the oxide thickness and V_{th} the threshold voltage. Therefore, from (5) and (6), the mean square value of the noise current contributed from $\Delta R(x_o)$ is then by [6]

$$\begin{aligned}\overline{\Delta i(x_o)^2} &= g_{DS}^2(x_o)\cdot\overline{\Delta v(x_o)^2} \\ &= -\frac{4kT(x_o)\Delta f W\mu_{eff}Q(x_o)\Delta x}{L_{elec}^2}.\end{aligned} \tag{8}$$

Note that (8) is only true for the region where the carriers do not travel at their saturation velocity and it cannot be applied to the velocity saturation region (region II in Fig. 1) because the Nyquist theory fails in that region [12].

There is also a debate about the temperature $T(x_o)$ in (8)-whether it is the electron temperature T_e or the lattice temperature T_o. Let us assume that $T(x_o)$ is the electron temperature. In this case, we can use the most commonly adopted equation for the electron temperature at the position x_o [19],

$$T_e(x_o) = T_o\left(1 + \delta\left(\frac{E(x_o)}{E_{cirt}}\right)^2\right), \tag{9}$$

where δ is a fitting parameter and its value is in the range of 5–20 for values of E_{crit} in the range of 2–4 V/μm [19]. The total noise spectral density $S_{i_d^2}$ from region I is then given by the integration of (8) from $x = 0$ to $x = L_{elec}$ divided by Δf which is

$$\begin{aligned}S_{i_d^2} &= \frac{\overline{i_d^2}}{\Delta f} = -\frac{4kT_o}{L_{elec}^2} \\ &\times \int_0^{L_{elec}}\left(1 + \delta\left(\frac{E(x_o)}{E_{crit}}\right)^2\right) W\mu_{eff}Q(x_o)dx\end{aligned} \tag{10}$$

where $\overline{i_d^2}$ is the mean square value of the total noise current. After rearranging the (10), the spectral density of the channel noise $S_{i_d^2}$ becomes

$$S_{i_d^2} = \frac{4kT_o}{L_{elec}^2}\mu_{eff}(-Q_{inv}) + \delta\frac{4kT_o I_D}{L_{elec}^2 E_{crit}^2}V_{DSsat} \tag{11}$$

where $-Q_{inv}$ is the total inversion charge in gradual channel region (region I). Equation (11) is general and can be applied to any compact model. Different complexity and accuracy will be achieved depending on the models used to calculate the inversion charge Q_{inv} and the channel length modulation effect ΔL. Note that V_{DSsat} in (11) will become V_{DS} and L_{elec} will become L_{eff} when the device operates in the linear mode. Equation (11) is similar to (10) in [10], but it uses the L_{elec} instead of L_{eff} for the noise calculation.

There have been two different approaches in the literature to calculate the total noise spectral density $S_{i_d^2}$ from region I. The first approach is to obtain the spectral density of the noise current from each channel section at the drain terminal and integrate each noise current density along the channel as described above [2], [6]. The other approach is to integrate each noise voltage density along the channel and then multiply the total spectral density of the noise voltage by the square of g_{DS} [4], [9]. For a linear resistor, the output conductance is independent of the location in the resistor, and the two approaches are essentially the same because the g_{DS}^2 can be taken out of the integration in (10). However, for a non–linear resistor like a MOSFET, the output conductance is a function of channel position x_o as shown in (6), and the second approach is essentially not correct. Therefore, in this brief, the channel noise from region I is calculated based on the first approach.

B. Channel Noise From the Velocity Saturation Region (Region II)

For the noise current generated from the velocity saturation region (region II), several models were presented in [4], [8]–[10] for example, to calculate the noise current from this region. For the noise models in [8] and [10], the equation based on the equation (8.5.18) in [6] for the model derivation is only true in the absence of velocity saturation [6]. On the other hand, because the Ohm's law is not valid in the velocity saturation region, the local resistance ΔR in (4) is not defined and therefore the thermal noise (or Johnson noise) theory can not be used in region II [12]. These reasons make the noise calculation in [4] questionable in region II.

The key question for the noise calculation in region II is what is the noise mechanism if the thermal noise theory fails? Different noise mechanisms – diffusion noise model [20], [21] and drifting dipole layer model [9], [12] have been proposed for the noise calculation in velocity saturation region. However, in this paper, we will show that there is no noise current generated from region II based on the following "thought" experiment. Let us assume that there exists a noise mechanism that generates a finite voltage fluctuation at a local position x_o in region II. Because the carriers in region II travel at their the saturation velocity, the carriers will not respond to the local change of the electric field caused by the noise voltage fluctuation. Therefore, there will be no noise current (or current fluctuation) generated by the finite noise voltage at the position x_o in the velocity saturation region. This applies to all the locations in region II, and therefore it is assumed that the noise current from region II is zero. This conclusion will be checked with experimental data.

III. Measurements and Discussions

The devices–under–tests (DUT) are fabricated in a 0.18 μm CMOS technology with channel width $W = 10 \times 6$ μm and channel lengths $L = 0.18$ μm, 0.42 μm and 0.97μm, respectively. Fig. 2 shows the extracted (symbols) and simulated (lines) spectral density of the channel noise $S_{i_d^2}$ versus V_{GS} characteristics for the n-type MOSFETs with

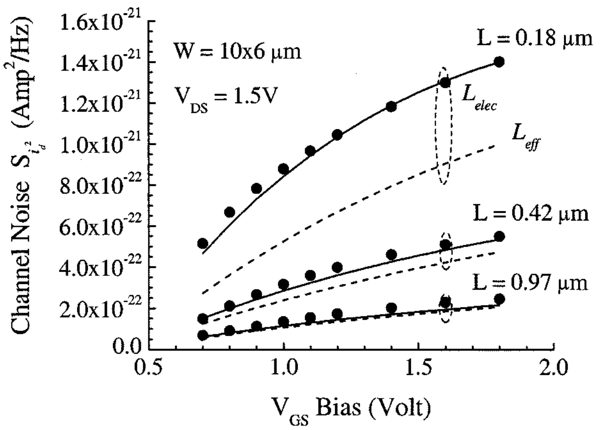

Fig. 2. Extracted (symbols) and simulated (lines) spectral density of the channel noise versus V_{GS} characteristics of the n-type MOSFETs with channel width $W = 10 \times 6$ μm and channel lengths $L = 0.97$ μm, 0.42 μm and 0.18 μm, respectively, biased at $V_{DS} = 1.5$ V with $\delta = 0$. The solid lines are obtained by using L_{elec} and the dashed lines are obtained by using L_{eff} in (11).

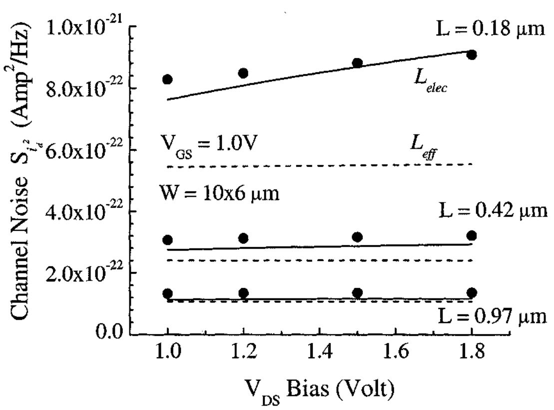

Fig. 3. Extracted (symbols) and simulated (lines) spectral density of the channel noise versus V_{DS} characteristics of the n-type MOSFETs with channel width $W = 10 \times 6$ μm and channel lengths $L = 0.97$ μm, 0.42 μm and 0.18 μm, respectively biased at $V_{GS} = 1.0$ V with $\delta = 0$. The solid lines are obtained by using L_{elec} and the dashed lines are obtained by using L_{eff} in (11).

channel width $W = 10 \times 6$ μm and channel lengths $L = 0.97$ μm, 0.42 μm and 0.18 μm, respectively biased at $V_{DS} = 1.5$ V and with $\delta = 0$. The inversion charge model in [18] is used to calculate the Q_{inv} in (11). The solid lines are obtained by using L_{elec} and the dashed lines are obtained by using L_{eff} in (11). It is shown that the CLM effect begins to have some impact on the channel noise when the channel length of the device is smaller than 0.5 μm, and that is why the simulated channel noise from region I in [10] predicts lower channel noise from 0.25 μm and 0.18 μm channel–length devices. Although [10] corrects this degradation by the introduction of the channel noise current caused by the hot electrons from the velocity saturation region, the equation used in the model derivation cannot be applied to the location where carriers travel at their saturation velocity, as discussed in Section II. Another observation from Fig. 2 is that the hot electron effects suggested in [2] and [22] and used in [3]–[5] and [10] does not show too much impact on the channel noise of deep submicron MOSFETs, in agreement with the conclusion in [7].

For the V_{DS} dependence of the channel noise, Fig. 3 shows extracted (symbols) and calculated (lines) spectral density of the channel noise $S_{i_d^2}$ versus V_{DS} characteristics for the n-type MOSFETs with channel width $W = 10 \times 6$ μm and channel lengths $L = 0.97$ μm, 0.42 μm

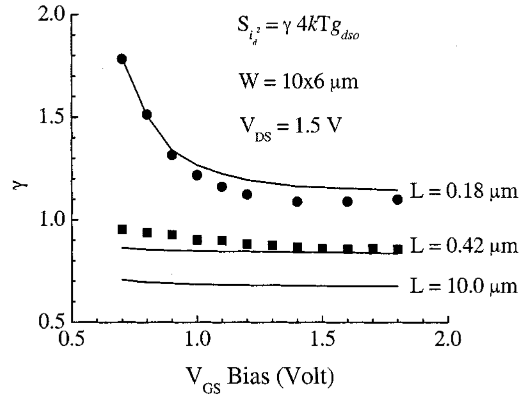

Fig. 4. Extracted (symbols) and simulated (lines) γ versus V_{GS} characteristics of the n-type MOSFETs with channel width $W = 10 \times 6$ μm and channel lengths $L = 10$ μm, 0.42 μm and 0.18 μm, respectively, biased at $V_{DS} = 1.5$ V with $\delta = 0$.

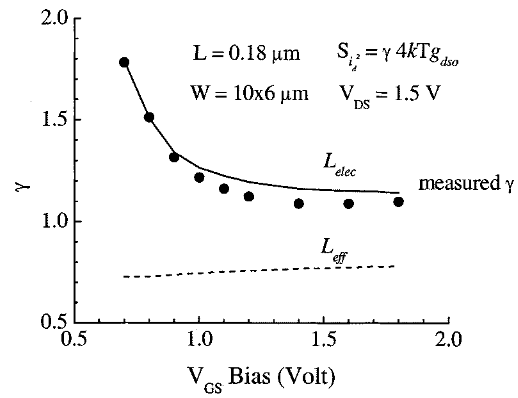

Fig. 5. Extracted (symbols) and simulated (lines) γ versus V_{GS} characteristics of the n-type NMOSFET with channel length $L = 0.18$ μm and width $W = 10 \times 6$ μm and biased at $V_{DS} = 1.5$ V with $\delta = 0$. The solid lines are obtained by using L_{elec}, and the dashed lines are obtained by using L_{eff} in (11).

and 0.18 μm, respectively biased at $V_{GS} = 1.0$ V and with $\delta = 0$. The solid lines are obtained by using L_{elec} and the dashed lines are obtained by using L_{eff} in the noise calculation. It is shown that the calculated channel noise using L_{eff} in (11) predicts lower channel noise, and cannot match the increasing trend of the extracted channel noise caused by the CLM effect for the deep submicron devices. The slope of simulated lines in the channel noise versus V_{DS} characteristics will depend on the accuracy of the model calculating the channel length modulation ΔL.

Sometimes, the spectral density of the channel noise is expressed as [2]

$$S_{i_d^2} = \gamma \cdot 4kTg_{dso} \tag{12}$$

where g_{dso} is the output conductance at zero drain bias (i.e., $V_{DS} = 0$). Based on the noise theory for long-channel devices, the value of γ is 2/3 [2]. However, when the channel length is reduced, the value of γ will be increased [7], [13]. Fig. 4 shows the extracted (symbols) and simulated (lines) γ versus V_{GS} characteristics of n-type MOSFETs with channel width $W = 10 \times 6$ μm and channel lengths $L = 10$ μm, 0.42 μm and 0.18 μm, respectively biased at $V_{DS} = 1.5$ V with $\delta = 0$. For the long-channel devices, the calculated γ is 0.68 at $V_{GS} = 1.8$ V, which agrees with the theoretical value. When the channel length is decreased, the γ value will increase from 0.68 to 1.2 or 1.8 (depending on the V_{GS} bias), and the model agrees well with the data. Fig. 5 shows the extracted (symbols) and simulated (lines) γ versus V_{GS} characteristics of the n-type MOSFET with channel length $L = 0.18\ \mu$m and width $W = 10 \times 6\ \mu$m and biased at $V_{DS} = 1.5$ V with $\delta = 0$. The solid line is obtained by using L_{elec} and the dashed line is obtained by using L_{eff}. It is shown again that the calculated γ using L_{eff} in (11) predicts lower γ value and cannot match the decreasing trend which is also reported in [7] when the V_{GS} bias is increased.

Finally, we want to discuss the impact of neglecting the velocity saturation effect in region I on the modeling of the channel noise and the accuracy of (11). As presented in Section II.A., (11) is derived based on the assumption that the electric field in the x direction for most of the sections in the gradual channel region is much less than the critical field E_{crit}. That is, we ignore the velocity saturation effect for sections in region I close to the boundary of regions I and II. If we include the velocity saturation effect in region I by modeling the local mobility with the empirical relation [2], [6], then

$$\mu(x_o) = \frac{\mu_{eff}}{1 + \frac{E(x_o)}{E_{crit}}} \tag{13}$$

with $E(x_o)$ being the electric field at the position x_o in region I and μ_{eff} being given by (7). Now the dc drain current I_{ds} becomes

$$\begin{aligned} I_{ds} &= \frac{W\mu_{eff}(-Q(x_o))}{1 + \frac{E(x_o)}{E_{crit}}} \cdot \frac{dV(x_o)}{dx} \\ &= \frac{\Delta V(x_o)}{\Delta R_{loc}(x_o)} \end{aligned} \tag{14}$$

where $\Delta R_{loc}(x_o)$ is the local channel resistance at the position x_o. It is difficult to derive an analytical expression for $\Delta R_{loc}(x_o)$ from (14), but it can be observed quantitatively that the local channel resistance is increased due to the velocity saturation effect (i.e., $\Delta R_{loc}(x_o) > \Delta R(x_o)$), and this implies that a higher thermal noise voltage is generated from the section at the position x_o close to L_{elec}. However, as can be seen from (6), the local output conductance $g_{DSloc}(x_o)$ at position x_o including the velocity saturation effect will be decreased because the local mobility $\mu(x_o)$ is reduced (i.e., $g_{DSloc}(x_o) < g_{DS}(x_o)$). The good matching obtained between the calculated $S_{i_d^2}$ using (11) and the extracted $S_{i_d^2}$ indicates that the product of $g_{DSloc}(x_o)^2 \cdot \Delta R_{loc}(x_o)$ is approximately about the same as $g_{DS}(x_o)^2 \cdot \Delta R(x_o)$ or the difference between these two products is negligible. This means that the impact of the velocity saturation effect in region I on the channel noise modeling is not as pronounced as that on the modeling of dc current, and it can be considered as a secondary effect compared to the CLM effect in the channel noise modeling of short–channel devices down to 0.18 μm.

IV. Conclusion

The channel length modulation (CLM) effect begins to have impact on the devices with channel length shorter than 0.5 μm. For deep submicron MOSFETs, if the CLM effect is not included, the calculated spectral density of the channel noise will be much lower than the experimental results. On the other hand, the noise contributions from the velocity saturation region and from the hot electron effect seem to be negligible in the channel noise modeling of deep submicron MOSFETs.

Acknowledgment

The authors would like to thank Dr. Y. Cheng and Dr. J. Zheng, Conexant Systems, Inc., Newport Beach, CA, and Dr. M. Matloubian, Mindspeed Technologies, Newport Beach, CA for their assistance in the device fabrication and RF noise measurements. They would also like to thank the reviewers for their useful comments and suggestions.

References

[1] D. K. Shaeffer and T. H. Lee, "A 1.5 V 1.5 GHz CMOS low noise amplifier," *IEEE J. Solid–State Circuits*, vol. 32, pp. 745–759, May 1997.

[2] A. van der Ziel, *Noise in Solid State Devices and Circuits*. New York: Wiley, 1986.

[3] P. A. Layman and S. G. Chamberlain, "A compact thermal noise model for the investigation of soft error rates in MOS VLSI Digital Circuits," *IEEE J. Solid–State Circuits*, vol. 24, pp. 79–89, Feb. 1989.

[4] D. P. Triantis, A. N. Birbas, and D. Kondis, "Thermal noise modeling for short–channel MOSFETs," *IEEE Trans. Electron Devices*, vol. 43, pp. 1950–1955, Nov. 1996.

[5] P. Klein, "An analytical thermal noise model of deep submicron MOSFETs," *IEEE Electron Device Lett.*, vol. 20, pp. 399–401, Aug. 1999.

[6] Y. P. Tsividis, *Operation and Modeling of the MOS Transistor*, 2nd ed. Englewood Cliffs, NJ: McGraw–Hill, 1999.

[7] A. J. Scholten, H. J. Tromp, L. F. Tiemeijer, R. van Langevelde, R. J. Havens, P. W. H. de Vreede, R. F. M. Roes, P. H. Woerlee, A. H. Montree, and D. B. M. Klaassen, "Accurate thermal noise model for deep–submicron CMOS," in *IEDM Tech. Dig.*, Dec. 1999, pp. 155–158.

[8] W. Jin, P. C. H. Chan, and J. Lau, "A physical thermal noise model for SOI MOSFET," *IEEE Trans. Electron Devices*, vol. 47, pp. 768–773, Apr. 2000.

[9] C. H. Park and Y. J. Park, "Modeling of thermal noise in short–channel MOSFETs at saturation," *Solid–State Electron.*, vol. 44, pp. 2053–2057, Nov. 2000.

[10] G. Knoblinger, P. Kelin, and M. Tiebout, "A new model for thermal channel noise of deep–submicron MOSFETs and its application in RF–CMOS design," *IEEE J. Solid–State Circuits*, vol. 36, pp. 831–837, May 2001.

[11] M. J. Deen, C. H. Chen, and Y. Chen, "MOSFET modeling for low noise, RF circuit design," in *IEEE Custom Integrated Circuits Conf. (CICC 2002)*, Orlando, FL, May 12–15, 2002, pp. 201–208.

[12] E. Statz, H. A. Haus, and R. A. Pucel, "Noise characteristics of gallium arsenide field–effect transistors," *IEEE Trans. Electron Devices*, vol. ED–21, pp. 549–562, Sept. 1974.

[13] C. H. Chen, M. J. Deen, Y. Cheng, and M. Matloubian, "Extraction of the induced gate noise, channel thermal noise and their correlation in sub–micron MOSFETs from RF noise measurements," *IEEE Trans. Electron Devices*, vol. 48, pp. 2884–2892, Dec. 2001.

[14] C. H. Chen and M. J. Deen, "High frequency noise of MOSFETs I – Modeling," *Solid–State Electron.*, vol. 42, pp. 2069–2081, Nov. 1998.

[15] K. Takeuchi and M. Fukuma, "Effects of the velocity saturated region on MOSFET characteristics," *IEEE Trans. Electron Devices*, vol. 41, pp. 1623–1627, Sept. 1994.

[16] P. K. Ko, R. S. Muller, and C. Hu, "A unified model for the hot–electron currents in MOSFETs," in *IEDM Tech. Dig.*, 1981, pp. 600–603.

[17] Y. Zhu, M. J. Deen, and T. M. Kleinpenning, "A New $1/f$ Noise model for metal–oxide–semiconductor field–effect transistors in saturation and deep saturation," *J. Appl. Phys.*, vol. 72, pp. 5990–5998, Dec. 1992.

[18] W. Liu, X. Jin, K. M. Cao, and C. Hu, *BSIM4.0.0 MOSFET Model Users' Manual*. Berkeley, CA: Univ. California, 2000.

[19] D. Gasquet, "Noise temperature and hot–carrier thermal conductivity in semiconductors," Ph.D., Univ. Montpellier II, Montpellier, France, 1995.

[20] A. van der Ziel and K. M. van Vliet, "H.F. thermal noise in space–charge limited solid state diodes – II," *Solid–State Electron.*, vol. 11, pp. 508–509, 1968.

[21] J.-P. Nougier, "Fluctuations and noise of hot carriers in semiconductor materials and devices," *IEEE Trans. Electron Devices*, vol. 41, pp. 2034–2049, Nov. 1994.

[22] A. van der Ziel, "Thermal noise in the hot electron regime in FETs," *IEEE Trans. Electron Devices*, vol. ED-18, pp. 977–977, Oct. 1971.